Available online at www.sciencedirect.com
ScienceDirect
Journal of Organometallic Chemistry 693 (2008) 1073–1080
Journal of Organometallic Chemistry
www.elsevier.com/locate/jorganchem

Iron(II) and cobalt(II) complexes bearing *N*-((pyridin-2-yl)methylene)-quinolin-8-amine derivatives: Synthesis and application to ethylene oligomerization

Kefeng Wang, Katrin Wedeking, Weiwei Zuo, Dongheng Zhang, Wen-Hua Sun *

Key Laboratory of Engineering Plastics and Beijing National Laboratory for Molecular Sciences, Institute of Chemistry, Chinese Academy of Sciences, Beijing 100080, China

Received 20 October 2007; received in revised form 23 December 2007; accepted 28 December 2007
Available online 8 January 2008

Abstract

A series of tridentate NˆNˆN iron(II) and cobalt(II) complexes containing *N*-((pyridin-2-yl)methylene)-quinolin-8-amine derivatives were synthesized and characterized by elemental and spectroscopic analyses. The molecular structure of **1a** was confirmed by X-ray diffraction analyses. On treatment with modified methylaluminoxane, these metal complexes exhibited good catalytic activities up to 2.8×10^6 g mol^{-1}(Fe) h^{-1} for ethylene oligomerization, and butenes were the major products with nice selectivity for 1-C_4. The steric and electronic effects on catalytic activities of metal complexes were carefully investigated as well as the influence of various reaction parameters. In the catalytic system, Fe(II) complexes performed better catalytic activities than their Co(II) analogues. With ligands having bulky substituents, the better catalytic activity was observed in catalytic system of Fe(II) complex, however, the lower catalytic activity was obtained in catalytic system of Co(II) complexes.

Keywords: Fe(II) and Co(II) complex; *N*-((Pyridin-2-yl)methylene)-quinolin-8-amine; Ethylene oligomerization

1. Introduction

The oligomerization of ethylene is currently the primary resource of linear α-olefins, which are important substances extensively used in the preparation of detergents, lubricants, plasticizers, oil chemicals and monomers for copolymerization. In recent years, substantive progress has been made in Fe(II) and Co(II) complexes bearing 2,6-bis(imino)pyridines as highly active catalysts by the groups of Brookhart [1] and Gibson [2]. Encouraged by that, many studies have been conducted for the effects of ligand environment on activity, selectivity and the property of the products [3]. Moreover, there have many efforts of chemists devoting to the development of tridentate Fe(II) and Co(II) catalysts [4], which were reviewed by the recent articles [5].

In devising late-transition metal complexes as catalysts for ethylene polymerization and oligomerization, our group recently reported series of tridentate NˆNˆN complexes (Scheme 1) with good to high activities for ethylene polymerization and oligomerization, in which the complexes contained ligands such as 2-imino-1,10-phenanthrolines (**A**) [6], 2-(benzoimidazolyl)-6-iminopyridines (**B**) [7], 2-quinoxalinyl-6-iminopyridines (**C**) [8], 2-(benzimidazol-2-yl)-1,10-phenanthrolines (**D**) [9], and 2-methyl-2,4-bis-(6-iminopyridin-2-yl)-*1H*-1,5-benzodiazepines (**E**) [10]. Indeed, those Fe(II) and Co(II) catalysts conducted ethylene oligomerization in high activities and high selectivity of 1-olefins, which could be promising catalysts in industrial consideration. Therefore, their derivatives have been synthesized and further investigations for better catalytic performances have been conducted through controlling

* Corresponding author. Tel.: +86 10 62557955; fax: +86 10 62618239.
E-mail address: whsun@iccas.ac.cn (W.-H. Sun).

0022-328X/$ - see front matter © 2008 Elsevier B.V. All rights reserved.
doi:10.1016/j.jorganchem.2007.12.030

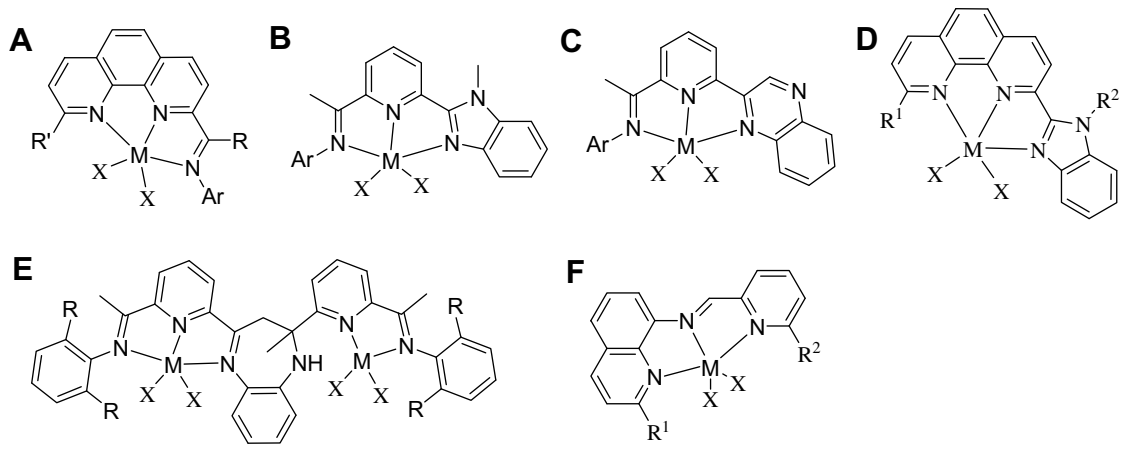

Scheme 1. Tridentate N^N^N catalysts.

steric and electronic effects of their ligands by modifying their substituents. Basically those existing catalytic models of Fe(II) and Co(II) complexes have been coordinated with various ligands centered of *N*-heteroaromatic ring. Instead, we are searching for an alternative model with ligands containing Schiff-base in center along with *N*-heteroaromatic rings. Therefore, this work deals with Fe(II) and Co(II) complexes ligated by *N*-((pyridin-2-yl)methylene)-quinolin-8-amine derivatives.

Actually the nickel complexes bearing *N*-((pyridin-2-yl)methylene)-quinolin-8-amine derivatives were synthesized and performed high catalytic activity in ethylene oligomerization [11]. Extensively, their Fe(II) and Co(II) analogues were synthesized in similar procedure. Their catalytic behaviors were carefully investigated with various reaction parameters along with the effects of substituents of the ligands. Herein we report the synthesis and characterization of the title complexes and their catalytic properties for ethylene oligomerization.

2. Results and discussions

2.1. Synthesis and characterization of the complexes

The substituted 8-aminoquinolines were synthesized according to literature procedures [12]. However, those compounds were not stable well for purification [11,13], one-pot template synthesis was employed in the synthesis of the Fe(II) and Co(II) complexes [14]. Closer to this work, their nickel analogues were synthesized using nickel template reaction [11]. Similarly, the template synthetic reaction of the 8-aminoquinoline derivative, pyridine-2-aldehyde derivative and $FeCl_2 \cdot 4H_2O$ or $CoCl_2$ were carried out in presence of acetic acid to afford the corresponding complexes (Scheme 2). The resulting products were precipitated from the reaction solution and collected by filter, washed with diethyl ether to remove acetic acid and dried in vacuum. The complexes were separated as air-stable powders in moderate to high yields, however, they will turn to purple in solution when exposed to air,

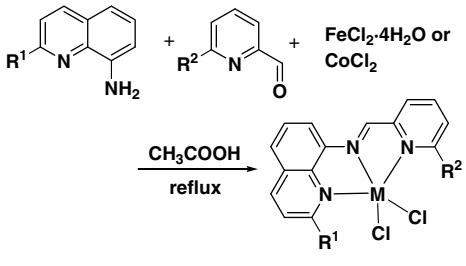

	1a	2a	3a	4a	5a	6a	7a
R^1	Me	H	Me	^{i}Pr	^{i}Pr	Cy	Cy
R^2	H	Me	Me	H	Me	H	Me
M	Fe	Fe	Fe	Fe	Fe	Fe	Fe

	1b	2b	3b	4b	5b	6b	7b
R^1	Me	H	Me	^{i}Pr	^{i}Pr	Cy	Cy
R^2	H	Me	Me	H	Me	H	Me
M	Co	Co	Co	Co	Co	Co	Co

Scheme 2. Synthesis of tridentate iron(II) and cobalt(II) complexes.

indicating their oxidation in solution. All complexes were characterized with elemental analysis and IR spectroscopy; In the IR spectra, strong and sharp band in the ranges of 1613–1624 cm^{-1} could be ascribed to the stretching vibration of C=N. Due to the paramagnetic nature of iron(II) and cobalt(II) complexes, the NMR data could not be obtained. To confirm their unambiguous structures, the single-crystal X-ray crystallography was employed to determine the molecular structure of **1a**.

2.2. Crystal structures

Previous research revealed that nickel complexes of the same framework could form either dimeric or monomeric structures in the solid state, depending on the bulk of the substitutes [11]. Herein the Fe(II) complex (**1a**) was confirmed to be monomeric one, though **1a** ($R^1 = Me$, $R^2 = H$) was the least bulky one of the series of complexes.

Crystals of **1a** suitable for X-ray structural determination were grown from a methanol solution through slowly evaporation of the solvent at room temperature. The molecular structure is shown in Fig. 1, whereas selected bond lengths and angles are listed in Table 1. The

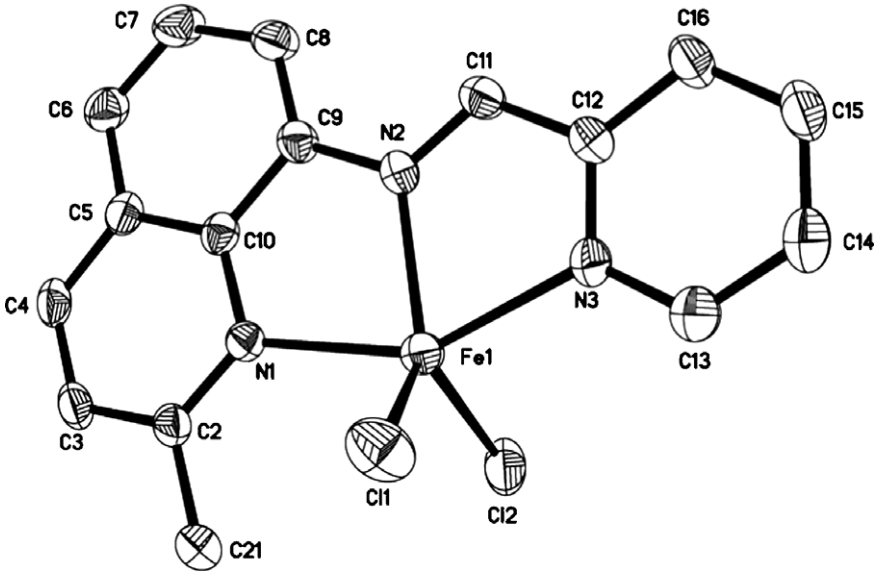

Figure 1. Molecular structure of **1a**, with thermal ellipsoids at the 30% probability level. Hydrogen atoms have been omitted for clarity.

Table 1
Selected bond lengths (Å) and angles (°) for **1a**

Bond length			
Fe(1)–N(1)	2.217(3)	Fe(1)–Cl(1)	2.3069(2)
Fe(1)–N(2)	2.122(3)	Fe(1)–Cl(2)	2.2972(2)
Fe(1)–N(3)	2.199(4)	N(2)-C(11)	1.284(5)
Bond angle			
N(2)–Fe(1)–N(1)	75.46(1)	N(3)–Fe(1)–Cl(1)	92.51(1)
N(2)–Fe(1)–N(3)	74.32(1)	N(1)–Fe(1)–Cl(2)	99.76(1)
N(1)–Fe(1)–N(3)	149.53(1)	N(2)–Fe(1)–Cl(2)	118.96(1)
N(1)–Fe(1)–Cl(1)	101.41(1)	N(3)–Fe(1)–Cl(2)	98.06(1)
N(2)–Fe(1)–Cl(1)	124.45(1)	Cl(1)–Fe(1)–Cl(2)	116.22(6)

coordination of the Fe-center can be described as distorted trigonal bipyramid geometry in which an equatorial plane is formed by the imine nitrogen (N(2)) and the two chlorides, while the nitrogen (N(1)) of the quinolyl group and the nitrogen (N(3)) of the pyridyl group are located in axial positions. As expected, the iron center coordinated with N1, N2 and N3 of the ligand, forming two fused five-membered rings with acute N–Fe–N angles: 75.46(1)° of N1–Fe1–N2 and 74.32(1)° of N2–Fe1–N3. The N(2)–C(11) bond distance is 1.284(5) Å, displaying typical C=N double bond character. The Fe–N bonds are different from each other. The shortest bond with 2.122(3) Å is found for the imine–N (Fe(1)–N(2)), followed by the pyridine–N with Fe(1)–N(3) of 2.199(4) Å and the quinoline–N with Fe(1)–N(1) of 2.217(3) Å. This trend is different from the monomeric structures of the nickel analogues [11], in which N(2)–Ni < N(1)–Ni < N(3)–Ni is observed. Moreover, the length of Fe–N bond is a little longer than the corresponding Ni–N bond [11]. The angle of Cl(1)–Fe(1)–Cl(2) is 116.22(6)°, which is obviously smaller than the nickel analogues [11]. Compared with other tridentate N^N^N iron(II) complexes [1,3e,6b,7a,9b,10], there is no much difference in the bond lengths and bond angles. However, not only Me group, but also Cy is smaller than 2,6-substituted aryl group, maybe it is why only short chain oligomers could be obtained (see Section 2.3) while other system [1,3e,6b,7a,10] could provide polymer along with long-chain oligomers. Similarly, other catalysts ligated by less bulky ligands also gave short chain oligomers [9b], indicating the importance of bulky substituent. The Fe–center deviates by 0.0788 Å out of the equatorial plane. The axial plane is almost vertical to the equatorial plane, with the dihedral angle of 87.7°. The ligand backbone of **1a** is not planar, having the dihedral angle of 4.9° between quinoline and pyridine ring.

2.3. Ethylene oligomerization

The Fe(II) and Co(II) complexes **1a**–**7a** and **1b**–**7b** were systematically investigated for ethylene oligomerization. Among the various aluminium activators, modified methylaluminoxane (MMAO) is the best one which exhibited catalytic activities in the order of 10^5–10^6 g mol^{-1}(M) h^{-1}. Therefore, MMAO was used as activator for further investigations. During ethylene oligomerization, ethylene consumption was smoothly kept on about 20 min. However, ethylene consumption decreased sharply after 20 min, suggesting partly deactivations of the active species. Butenes predominate among the produced oligomers, with moderate to good selectivity for 1-C_4. Since the low content of C_6 and several isomers of C_6 detected, it is difficult to quantify the individual isomer accurately. However, the selectivity for 1-C_6 is low. Compared with the nickel analogues [11], the Fe(II) and Co(II) complexes containing *N*-((pyridin-2-yl)methylene)-quinolin-8-amine derivatives showed comparable activities and selectivities, indicating that the late-transition metal complexes (Fe(II),

Co(II) and Ni(II)) bearing these series of ligand could exhibit good catalytic performance in ethylene oligomerization. Moreover, if compared with other bidentate Fe(II) and Co(II) catalysts [15], the series of complexes exhibit much better catalytic performance, not only in activity, but also in selectivity.

2.3.1. Effects of reaction parameters on catalytic behavior of iron complexes

Complex **5a** was typically investigated in detail under a range of reaction conditions, such as molar ratio of cocatalyst to catalyst, reaction temperature and pressure. The oligomerization results are summarized in Table 2. As revealed in Table 2, the reaction parameters significantly affect the catalytic activity and selectivity; however, no obvious influence on the product distribution could be observed.

With complex **5a**, the amount of MMAO played an important role on the catalytic performance. Increasing the Al/Fe molar ratio from 500 to 2000 (entries 1–4 in Table 2), the catalytic activity of **5a** increased obviously and the highest activity (27.7×10^5 g mol^{-1}(Fe) h^{-1}, entry 4 in Table 2) was observed at Al/Fe ratio of 2000, which may be attributed to the fact that MMAO scavenged adventitious water and impurities in the solvent at low Al/Fe ratio and the iron complex required more cocatalyst to be activated. However, when Al/Fe molar ratio was further increased (entry 5 in Table 2), the activity decreased. The decrease in oligomerization activity might be caused by the impurities in commercial MMAO such as alkyl aluminium, which led to the deactivation of active catalytic sites [3b]. Though the activity was sensitive to the Al/Fe ratio, the selectivity for 1-C_4 kept stable in different ratios, and higher activity could not result in oligomers longer than C_6.

When Al/Fe molar ratio of 2000 was fixed, the reaction temperature significantly affects the catalytic activity. Elevation of the temperature from 20 °C to 60 °C (entries 6 and 7 in Table 2) led to a significant decline in activity; indicating that the catalyst is not stable in higher temperature, another reason could be attributed to lower ethylene solubility at higher temperature. Moreover, the selectivity for 1-C_4 decreased sharply at elevated temperatures, (entries 6 and 7 in Table 2) indicating that isomerization is favored in higher temperatures.

Ethylene oligomerization of complex **5a** was also carried out at different pressures (entries 8 and 9 in Table 2). As expected, the higher pressure, the higher catalytic activity. In 10 atm, the activity decreased to about 1/7 of the value in 30 atm. The catalytic activities predominantly decreased at lower ethylene pressure, due to lower monomer concentration at lower pressure. With higher temperatures or lower pressure, the content of C_6 became higher; such phenomenon was reported in some complexes [3h,6h,11].

2.3.2. Effect of the ligand environment on the catalytic behavior of Fe(II) complexes

To compare the effect of ligand environment, complexes **1a**–**7a** were examined for oligomerization of ethylene under the same condition (20 °C; Al/Fe = 2000; 30 atm) and the results are summarized in Table 3. The substitution pattern of the ligand plays a major role on the performance of the catalysts.

The substituents R^1 and R^2 have considerable effects on the catalytic behaviors. For complexes **1a**–**3a**, the best activity and selectivity for 1-C_4 was obtained with **3a** (18.2×10^5 g mol^{-1}(Fe) h^{-1}, entry 3, Table 3), indicating that, higher activity and selectivity could be realized by introducing bulkier substituent to the ligand framework.

Furthermore, changing the R^1 substituent from Me to *i*-Pr or Cy while keeping the R^2 = Me, higher activities were observed and the highest activity of 28.3×10^5 g mol^{-1}(Fe) h^{-1} (entry 7 in Table 3) was obtained with the most bulky complexes **7a**. And for complex **5a**, the activity of 27.7×10^5 g mol^{-1}(Fe) h^{-1} (entry 5 in Table 3) was observed. A possible explanation is that the active site of the catalyst is protected by bulky substituents, leading to increase in activities. However, when the R^2 substituent is less bulky, the activity of its complex became apparently lower. For example, complex **5a** gave much higher activity ($27.7 \times 10^{5-1}$(Fe) h^{-1}, entry 5 in Table 3) than complex **4a** (6.9×10^5 g mol^{-1}(Fe) h^{-1}, entry 4 in Table 3). Such

Table 2
Oligomerization of ethylene with **5a**/MMAO[a]

Entry	Al/Fe	*T* (°C)	*P* (atm)	Oligomer distribution (%)[b]			Activity 10^5 g mol^{-1}(Fe) h^{-1}
				C_4	1-C_4	C_6	
1	500	20	30	95.7	95.7	4.3	3.8
2	1000	20	30	96.9	92.1	3.1	8.2
3	1500	20	30	99.5	93.3	0.5	17.3
4	2000	20	30	97.9	97.6	2.1	27.7
5	2500	20	30	98.3	89.9	1.7	10.4
6	2000	40	30	83.2	73.2	16.8	3.4
7	2000	60	30	82.7	72.3	17.3	2.2
8	2000	20	20	89.1	50.7	10.9	6.1
9	2000	20	10	85.4	82.6	14.6	3.7

[a] General conditions: 5 μmol of complex; 100 ml of toluene; 20 min.
[b] Weight percentage determined by GC.

Table 3
Ethylene oligomerization with **1a**–**7a**/MMAO[a]

Entry	Catalyst	Oligomer distribution (%)[b]			Activity 10^5 g mol^{-1}(Fe) h^{-1}
		C_4	1-C_4	C_6	
1	**1a**	99.1	93.6	0.9	12.1
2	**2a**	99.0	87.6	1.0	17.2
3	**3a**	98.5	96.6	1.5	18.2
4	**4a**	88.1	79.8	11.9	6.9
5	**5a**	97.9	97.6	2.1	27.7
6	**6a**	98.4	50.5	1.6	6.4
7	**7a**	98.9	98.2	1.1	28.3

[a] General conditions: 5 μmol of complex; 100 ml of toluene; 20 min; 20 °C; MMAO, Al/Fe = 2000; 30 atm.
[b] Weight percentage determined by GC.

phenomenon was also reported in other complexes [9b]. Nevertheless, for complex **4a**, the content of C_6 is higher.

As to the selectivity for 1-C_4, the complexes with bulky substituents both on R^1 and R^2 showed good result, higher than 90%. Comparison of complexes **4a** and **5a** (entries 4 and 5 in Table 3), it could be observed that **5a** exhibited not only better activity, but also better selectivity, suggesting that protection from R^1 and R^2 position is necessary for high activity and selectivity. Comparison of complexes **6a** and **7a** (entries 6 and 7 in Table 3) could give the same conclusion.

Compared with the analogue nickel complexes [11], the catalytic performances of the Fe(II) complexes in activity, selectivity and product distributions were observed to be similar. However, the influence of substituents on activity and selectivity is different from the nickel analogues.

2.3.3. Catalytic behavior of Co(II) complexes

Although in most cases, the cobalt(II) complexes showed much lower activities than their iron(II) analogues under similar reaction conditions, there are some reports in which comparable performance was observed with cobalt(II) complexes in comparison with its iron(II) analogues [3d,6h].

In our system, complexes **1b**–**7b** were examined under optimized conditions for oligomerization of ethylene with MMAO as the cocatalyst and the results are summarized in Table 4. It could be observed that the cobalt(II) complexes showed comparable activities with their iron(II) analogues for ethylene oligomerization. Complexes **4b** and **6b** even showed better activities than complexes **4a** and **6a**, respectively (entries 4 and 6 in Table 4). However, detailed comparison revealed that there are some differences in the catalytic properties from the iron(II) complexes. One is that all of the cobalt(II) complexes exhibit good selectivity for 1-C_4, regardless of the substituents bulkiness, which is quite different with the iron(II) analogues but in line with the nickel analogues [11]. Secondly, the highest activity, 22.8×10^5 g mol^{-1}(Co) h^{-1}, was obtained by the least bulky complex **1b** (entry 1 in Table 4). With bulkier complexes **5b**, lower activity was obtained (13.9×10^5 g mol^{-1} (Co) h^{-1}, entry 5, Table 4). Similar performance was also observed for another bulky complex **7b**, which showed activity as low as 18.5×10^5 g mol^{-1}(Co) h^{-1} (entry 7, Table 4). A possible explanation is that the active site of the catalyst is blocked by bulky substituents, leading to decrease in activities. Similar tendency had been observed for the nickel analogues [11] and other reported iron(II) complexes [6h].

Furthermore, the effects of catalyst concentration and ethylene pressure were also investigated by employing complex **1b**. At lower ethylene pressure, its activity obviously decreased (entry 8 to entry 1, Table 4), which was in line with its Fe(II) analogue. The higher catalyst concentration, the lower catalytic activity (entry 9 to entry 1, Table 4). That was caused by having less chance for active species to coordinate ethylene for further reaction.

Table 4
Ethylene oligomerization with **1b**–**7b**/MMAO[a]

Entry	Catalyst	Oligomer distribution (%)[b]			Activity 10^5 g mol^{-1}(Co) h^{-1}
		C_4	1-C_4	C_6	
1	**1b**	96.9	95.9	3.1	22.8
2	**2b**	97.2	96.3	2.8	17.8
3	**3b**	96.4	94.9	3.6	22.2
4	**4b**	96.2	95.2	3.8	15.1
5	**5b**	99.2	84.2	0.8	13.9
6	**6b**	96.7	95.2	3.3	8.5
7	**7b**	98.2	97.5	1.8	18.5
8[c]	**1b**	97.4	93.7	2.6	10.9
9[d]	**1b**	96.8	96.1	3.2	15.5

[a] General conditions: 5 μmol of complex; 100 ml of toluene; 20 min; 20 °C; MMAO, Al/Co = 1500; 30 atm.
[b] Weight percentage determined by GC.
[c] 20 atm.
[d] 10 μmol of complex **1b**.

3. Conclusions

A series of tridentate (NˆNˆN) Fe(II) and Co(II) complexes of *N*-((pyridin-2-yl)methylene)-quinolin-8-amine derivatives have been synthesized and fully characterized. These complexes were synthesized by metal template reaction. X-ray crystallographic analysis revealed that the Fe(II) complex forms monomeric structure with distorted trigonal bipyramid geometry. Activated with MMAO, all the Fe(II) complexes exhibited high catalytic activities up to 10^6 g mol^{-1}(M) h^{-1} for ethylene oligomerization with dimers and trimers as products. The selectivity for 1-C_4 is moderate to high. Bulky substituents resulted in both good activity and selectivity for 1-C_4. Catalytic reaction parameters significantly affect the catalytic activity and higher temperature or lower pressure brought lower activities. The Co(II) complexes also showed good catalytic activity and selectivity comparable with Fe(II) analogues. However, the influence of substituents is different from the Fe(II) analogues and less bulky substituents resulted in better activity. This research confirmed that late-transition metal complexes (Ni, Fe and Co) ligated by *N*-((pyridin-2-yl)methylene)-quinolin-8-amine derivatives exhibit good catalytic performance in ethylene oligomerization. Therefore, the Schiff-base centered tridentate ligands could provide alternative catalytic models and are worthy of further investigation for highly active performance.

4. Experimental

4.1. General considerations

All manipulations of air and/or moisture-sensitive compounds were carried out under an atmosphere of nitrogen using standard Schlenk techniques. Solvents were refluxed over an appropriate drying agent, distilled and degassed before using. Methylaluminoxane (MAO, 1.46 M in

toluene) and modified methylaluminoxane (MMAO, 1.93 M in heptane) were purchased from Akzo Corp (USA). Substituted 8-nitro-quinolines and 8-aminoquinolines were prepared according to literature procedures [12]. High purity ethylene was purchased from Beijing Yanshan Petrochemical Co. and used as received. Other reagents were purchased from Aldrich, Acros or local supplier. Elemental analyses were performed on a Flash EA 1112 microanalyzer. IR spectra were recorded on a Perkin–Elmer System 2000 FT-IR spectrometer using KBr disc in the range of 4000–400 cm^{-1}. The ^1H NMR spectra were recorded on a Bruker DMX-300 instrument with TMS as the internal standard. GC analysis was performed with a VARIAN CP-3800 gas chromatograph equipped with a flame ionization detector and a 30 m (0.25 mm i.d., 0.25 μm film thickness) CP-Sil 5 CB column.

4.2. Synthesis of complexes

General procedure. Complexes **1a**–**7a** were prepared by using our previous procedure [11] (Scheme 2). A suspension of pyridine-2-aldehyde derivative (1.00 mmol), 8-aminoquinoline derivative (1.00 mmol), and $FeCl_2 \cdot 4H_2O$ (1.00 mmol) in glacial acetic acid (10 ml) was refluxed for 4 h. The precipitate was collected by filtration and washed with diethyl ether (3 × 5 ml). After washing, the collected solid was dried in vacuum.

Complex **1a** was obtained as a deep green powder in 87.2% yield. M.p: 258 °C (dec.). Anal. Calc. for $C_{16}H_{13}Cl_2N_3Fe \cdot 0.5H_2O$: C, 50.17; H, 3.68; N, 10.97. Found: C, 50.56; H, 3.50; N, 11.18%. IR (KBr; cm^{-1}): 3340, 3192, 1619, 1594, 1570, 1504, 1471, 1440, 1376, 1321, 1295, 1223, 1149, 1033, 847, 761.

Complex **2a** was obtained as a deep green powder in 81.7% yield. M.p: 244 °C (dec.). Anal. Calc. for $C_{16}H_{13}Cl_2N_3Fe \cdot 0.5H_2O$: C, 50.17; H, 3.68; N, 10.97. Found: C, 49.84; H, 3.51; N, 10.89%. IR (KBr; cm^{-1}): 3397, 3261, 1623, 1592, 1503, 1464, 1381, 1318, 1254, 1168, 1131, 1074, 1032, 832, 784.

Complex **3a** was obtained as a deep green powder in 80.7% yield. M.p: 254 °C (dec.). Anal. Calc. for $C_{17}H_{15}Cl_2N_3Fe \cdot 0.5H_2O$: C, 51.42; H, 4.06; N, 10.58. Found: C, 51.00; H, 3.88; N, 10.08%. IR (KBr; cm^{-1}): 3332, 3188, 1618, 1592, 1502, 1464, 1434, 1381, 1321, 1254, 1218, 1145, 1039, 841, 763.

Complex **4a** was obtained as a deep green powder in 52.3% yield. M.p: >300 °C. Anal. Calc. for $C_{18}H_{17}Cl_2N_3Fe \cdot H_2O$: C, 51.46; H, 4.56; N, 10.00. Found: C, 51.71; H, 4.19; N, 10.07%. IR (KBr; cm^{-1}): 3057, 2968, 2867, 1613, 1593, 1567, 1505, 1457, 1373, 1297, 1227, 1150, 1044, 848, 766.

Complex **5a** was obtained as a deep green powder in 51.6% yield. M.p: >300 °C. Anal. Calc. for $C_{19}H_{19}Cl_2N_3Fe \cdot 1.5H_2O$: C, 51.50; H, 5.00; N, 9.48. Found: C, 51.72; H, 4.28; N, 9.60%. IR (KBr; cm^{-1}): 3063, 2967, 2864, 1618, 1588, 1504, 1460, 1382, 1252, 1217, 1038, 844, 775.

Complex **6a** was obtained as a deep green powder in 92.9% yield. M.p: >300 °C. Anal. Calc. for $C_{21}H_{21}Cl_2N_3Fe \cdot 0.5H_2O$: C, 55.90; H, 4.91; N, 9.31 Found: C, 55.48; H, 4.64; N, 9.18%. IR (KBr; cm^{-1}): 2925, 2853, 1614, 1593, 1568, 1541, 1506, 1472, 1445, 1382, 1319, 1296, 1145, 998, 840, 767.

Complex **7a** was obtained as a deep green powder in 72.3% yield. M.p: >300 °C. Anal. Calc. for $C_{22}H_{23}Cl_2N_3Fe \cdot 0.5H_2O$: C, 56.80; H, 5.20; N, 9.03. Found: C, 56.39; H, 5.05; N, 8.62%. IR (KBr; cm^{-1}): 1621, 1592, 1570, 1504, 1460, 1446, 1387, 1319, 994, 840, 766.

General procedure. Complexes **1b**–**7b** were prepared in a similar procedure [11] by using $CoCl_2$ (Scheme 2). A suspension of pyridine-2-aldehyde derivative (1.00 mmol), 8-aminoquinoline derivative (1.00 mmol), and $CoCl_2$ (1.00 mmol) in glacial acetic acid (20 ml) was refluxed for 4 h. The precipitate was collected by filtration, washed with diethyl ether (3 × 5 ml). The resulting solid was dried in vacuum.

Complex **1b** was obtained as a yellow powder in 89.1% yield. M.p: >300 °C. Anal. Calc. for $C_{16}H_{13}Cl_2N_3Co$: C, 50.96; H,3.47; N, 11.14. Found: C, 50.71; H, 3.56; N, 11.15%. IR (KBr; cm^{-1}): 3446, 3058, 3020, 1618, 1593, 1571, 1506, 1474, 1443, 1370, 1294, 1222, 1152, 1013, 854, 772, 760.

Complex **2b** was obtained as a yellow powder in 79.2% yield. M.p: >300 °C. Anal. Calc. for $C_{16}H_{13}Cl_2N_3Co$: C, 50.96; H,3.47; N, 11.14. Found: C, 50.62; H, 3.29; N, 11.10%. IR (KBr; cm^{-1}): 3419, 3039, 1621, 1595, 1503, 1463, 1398, 1382, 1254, 1004, 965, 835, 785, 762.

Complex **3b** was obtained as a brown powder in 80.5% yield. M.p: >300 °C. Anal. Calc. for $C_{17}H_{15}Cl_2Co \cdot 0.5H_2O$: C, 51.02; H, 4.03; N, 10.50. Found: C, 50.97; H, 3.69; N, 10.19%. IR (KBr; cm^{-1}): 3445, 3063, 1618, 1590, 1505, 1462, 1382, 1254, 1216, 1168, 1003, 842, 791, 764, 736.

Complex **4b** was obtained as a brown powder in 72.3% yield. M.p: >300 °C. Anal. Calc. for $C_{18}H_{17}Cl_2N_3Co \cdot H_2O$: C, 51.08; H, 4.53; N, 9.93. Found: C,51.43; H, 4.22; N, 9.87%. IR (KBr; cm^{-1}): 3444, 1617, 1595, 1571, 1506, 1471, 1373, 1043, 1012, 844, 770.

Complex **5b** was obtained as a brown powder in 79.7% yield. M.p: >300 °C. Anal. Calc. for $C_{19}H_{19}Cl_2N_3Co$: C, 54.44; H, 4.57; N, 10.02. Found: C, 54.73; H, 4.22; N, 9.99%. IR (KBr; cm^{-1}): 3367, 3051, 2962, 1619, 1597, 1571, 1505, 1374, 1223, 1040, 841, 769.

Complex **6b** was obtained as a brown powder in 83.2% yield. M.p: >300 °C. Anal. Calc. for $C_{21}H_{21}Cl_2N_3Co$: C, 56.65; H, 4.75; N, 9.44. Found: C, 56.19; H, 4.78; N, 9.36%. IR (KBr; cm^{-1}): 3058, 1617, 1593, 1569, 1504, 1473, 1445, 1376, 1300, 1245, 1221, 1150, 842, 767.

Complex **7b** was obtained as a brown powder in 83.2% yield. M.p: >300 °C. Anal. Calc. for $C_{22}H_{23}Cl_2N_3Co$: C, 57.53; H, 5.05; N, 9.15. Found: C, 57.33; H, 5.04; N, 8.67%. IR (KBr; cm^{-1}): 1624, 1594, 1568, 1503, 1471, 1427, 1398, 1319, 1252, 1213, 1136, 1110, 1076, 1006, 828.

Table 5
Summary of crystallographic data for **1a**

Formula	$C_{16}H_{13}Cl_2FeN_3$
F_w	374.04
Crystal system	Monoclinic
Space group	$P2_1/c$
a (Å)	11.673(2)
b (Å)	10.094(2)
c (Å)	13.628(3)
β (°)	93.50(3)
V (Å^3)	1602.6(5)
Z	4
D_{calc} (g cm^{-3})	1.550
Absorption coefficient, μ (mm^{-1})	1.272
$F(000)$	760
θ Range (°)	2.51–27.48
Number of data collected	6823
Number of unique data	3664
Goodness-of-fit	1.069
R	0.0661
R_w	0.1432

4.3. Procedure for oligomerization of ethylene

High-pressure ethylene oligomerization was performed in a stainless steel autoclave (0.5 L capacity) equipped with gas ballast through a solenoid clave for continuous feeding of ethylene at constant pressure. A 100 mL amount of toluene containing the catalyst precursor was transferred to the fully dried reactor under a nitrogen atmosphere. The required amount of cocatalyst was then injected into the reactor using a syringe. As the prescribed temperature was reached, the reactor was pressurized to the desired pressure. After the reaction mixture was stirred for the desired period of time, the reaction was stopped and about 1 mL of the reaction solution was collected, quenched by the addition of 10% aqueous hydrogen chloride and then analyzed by gas chromatography (GC).

4.4. X-ray crystallographic studies

Single-crystal X-ray study for complex **1a** was carried out on a Rigaku R-AXIS Rapid IP diffractometer with graphite-monochromated Mo Kα radiation ($\lambda = 0.71073$ Å) at 296(2) K. Cell parameters were obtained by global refinement of the positions of all collected reflections. Intensities were corrected for Lorentz and polarization effects and empirical absorption. The structures were solved by direct methods and refined by full-matrix least-squares on F^2. All non-hydrogen atoms were refined anisotropically. All hydrogen atoms were placed in calculated positions. Structure solution and refinement were performed by using the SHELXL-97 package [16]. Crystal data and processing parameters for complex **1a** are summarized in Table 5.

Supplementary material

CCDC 661233 contains the supplementary crystallographic data for compound **1a**. These data can be obtained free of charge from The Cambridge Crystallographic Data Centre via www.ccdc.cam.ac.uk/data_request/cif.

Acknowledgements

This work was supported by NSFC No. 20674089 and MOST No. 2006AA03Z553.

References

[1] B.L. Small, M. Brookhart, A.M.A. Bennett, J. Am. Chem. Soc. 120 (1998) 4049–4050.
[2] G.J.P. Britovsek, V.C. Gibson, S.J. McTavish, G.A. Solan, A.J.P. White, D.J. Williams, B.S. Kimberley, P.J. Maddox, Chem. Commun. (1998) 849–850.
[3] (a) B.L. Small, M. Brookhart, J. Am. Chem. Soc. 120 (1998) 7143–7144;
(b) G.J.P. Britovsek, M. Bruce, V.C. Gibson, B.S. Kimberley, P.J. Maddox, S. Mastroianni, S.J. McTavish, C. Redshaw, G.A. Solan, S. Stromberg, A.J.P. White, D.J. Williams, J. Am. Chem. Soc. 121 (1999) 8728–8740;
(c) G.J.P. Britovsek, S. Mastroianni, G.A. Solan, S.P.D. Baugh, C. Redshaw, V.C. Gibson, A.J.P. White, D.J. Williams, M.R.J. Elsegood, Chem. Eur. J. 6 (2000) 2221–2231;
(d) W.-H. Sun, X. Tang, T. Gao, B. Wu, W. Zhang, H. Ma, Organometallics 23 (2004) 5037–5047;
(e) Y. Chen, R. Chen, C. Qian, X. Dong, J. Sun, Organometallics 22 (2003) 1231–1236;
(f) F.A.R. Kaul, G.T. Puchta, G.D. Frey, E. Herdtweck, W.A. Herrmann, Organometallics 26 (2007) 988–999;
(g) S. Mctavish, G.J.P. Britovsek, T.M. Smit, V.C. Gibson, A.J.P. White, D.J. Williams, J. Mol. Catal. A 261 (2007) 293–300;
(h) N. Ajellal, M.C.A. Kuhn, A.D.G. Boff, M. Hörner, C. M Thomas, J.-F. Carpentier, O.L. Casagrande, Organometallics 25 (2006) 1213–1216;
(i) C. Zhang, W.-H. Sun, Z.-X. Wang, Eur. J. Inorg. Chem. (2006) 4895–4902;
(j) Y.-M. Zhang, Q. Lin, T.-B. Wei, D.-H. Zhang, S.-Y. Jie, Inorg. Chim. Acta 358 (2005) 4423–4430;
(k) X. Tang, W.-H. Sun, T. Gao, J. Hou, J. Chen, W. Chen, J. Organomet. Chem. 690 (2005) 1570–1580.
[4] (a) M. Qian, M. Wang, R. He, J. Mol. Catal. A 160 (2000) 243–247;
(b) M. Qian, M. Wang, B. Zhou, R. He, Appl. Catal. A 209 (2001) 11–15;
(c) L. LePichon, D.W. Stephan, X. Gao, Q. Wang, Organometallics 21 (2002) 1362–1366;
(d) C. Bianchini, G. Mantovani, A. Meli, F. Migliacci, F. Laschi, Organometallics 22 (2003) 2545–2547;
(e) M.-S. Zhou, S.-P. Huang, L.-H. Weng, W.-H. Sun, D.-S. Liu, J. Organomet. Chem. 665 (2003) 237–245;
(f) G.J.P. Britovsek, V.C. Gibson, O.D. Hoarau, S.K. Spitzmesser, A.J.P. White, D.J. Williams, Inorg. Chem. 42 (2003) 3454–3465;
(g) R. Cowdell, C.J. Davies, S.J. Hilton, J.-D. Maréchal, G.A. Solan, O. Thomas, J. Fawcett, Dalton Trans. (2004) 3231–3240;
(h) C. Bianchini, D. Gatteschi, G. Giambastiani, I.G. Rios, A. Ienco, F. Laschi, C. Mealli, A. Meli, L. Sorace, A. Toti, F. Vizza, Organometallics 26 (2007) 726–739;
(i) B.L. Samll, R. Rios, E.R. Fernandez, M.J. Carney, Organometallics 26 (2007) 1744–1749;
(j) C. Görl, H.G. Alt, J. Mol. Catal. A 273 (2007) 118–132.
[5] (a) S.D. Ittel, L.K. Johnson, M. Brookhart, Chem. Rev. 100 (2000) 1169–1203;
(b) S. Mecking, Angew. Chem. Int. Ed. 40 (2001) 534–540;
(c) V.C. Gibson, S.K. Spitzmesser, Chem. Rev. 103 (2003) 283–315;
(d) W. Zhang, W. Zhang, W.-H. Sun, Prog. Chem. 17 (2005) 310–319;

(e) S. Jie, S. Zhang, W.-H. Sun, Petrochem. Tech. (Shiyou Huagong) 35 (2006) 295–300;
(f) W.-H. Sun, D. Zhang, S. Zhang, S. Jie, J. Hou, Kinet. Catal. 47 (2006) 278–283;
(g) C. Bianchini, G. Giambastiani, I.G. Rios, G. Mantovani, A. Meli, A.M. Segarra, Coord. Chem. Rev. 250 (2006) 1391–1418;
(h) V.C. Gibson, C. Redshaw, G.A. Solan, Chem. Rev. 107 (2007) 1745–1776.

[6] (a) L. Wang, W.-H. Sun, L. Han, H. Yang, Y. Hu, X. Jin, J. Organomet. Chem. 658 (2002) 62–70;
(b) W.-H. Sun, S. Jie, S. Zhang, W. Zhang, Y. Song, H. Ma, J. Chen, K. Wedeking, R. Fröhlich, Organometallics 25 (2006) 666–677;
(c) W.-H. Sun, S. Zhang, S. Jie, W. Zhang, Y. Li, H. Ma, J. Chen, K. Wedeking, R. Fröhlich, J. Organomet. Chem. 691 (2006) 4196–4203;
(d) S. Jie, S. Zhang, K. Wedeking, W. Zhang, H. Ma, X. Lu, Y. Deng, W.-H. Sun, C.R. Chim. 9 (2006) 1500–1509;
(e) S. Jie, S. Zhang, W.-H. Sun, X. Kuang, T. Liu, J. Guo, J. Mol. Catal. A: Chem. 269 (2007) 85–96;
(f) S. Zhang, S. Jie, Q. Shi, W.-H. Sun, J. Mol. Catal. A: Chem. 276 (2007) 174–183;
(g) J.D.A. Pelletier, Y.D.M. Champouret, J. Cadarso, L. Clowes, M. Gañete, K. Singh, V. Thanarajasingham, G.A. Solan, J. Organomet. Chem. 691 (2006) 4114–4123;
(h) S. Jie, S. Zhang, W.-H. Sun, Eur. J. Inorg. Chem. (2007) 5584–5598.

[7] (a) W.-H. Sun, P. Hao, S. Zhang, Q. Shi, W. Zuo, X. Tang, X. Lu, Organometallics 26 (2007) 2720–2734;
(b) P. Hao, S. Zhang, W.-H. Sun, Q. Shi, S. Adewuyi, X. Lu, P. Li, Organometallics 26 (2007) 2439–2446;
(c) Y. Chen, W. Zuo, P. Hao, S. Zhang, K. Gao, W.-H. Sun, J. Organomet. Chem., in press, doi:10.1016/j.jorganchem.2007.11.049.

[8] (a) W.-H. Sun, P. Hao, G. Li, S. Zhang, W. Wang, J. Yi, M. Asma, N. Tang, J. Organomet. Chem. 692 (2007) 4506–4518;
(b) S. Adewuyi, G. Li, S. Zhang, W. Wang, P. Hao, W.-H. Sun, N. Tang, J. Yi, J. Organomet. Chem. 692 (2007) 3532–3541.

[9] (a) M. Zhang, S. Zhang, P. Hao, S. Jie, W.-H. Sun, P. Li, X. Lu, Eur. J. Inorg. Chem. (2007) 3816–3826;
(b) M. Zhang, P. Hao, W. Zuo, S. Jie, W.-H. Sun, J. Organomet. Chem. 693 (2008) 483–491.

[10] (a) S. Zhang, I. Vystorop, Z. Tang, W.-H. Sun, Organometallics 26 (2007) 2456–2460;
(b) S. Zhang, W.-H. Sun, X. Kuang, I. Vystorop, J. Yi, J. Organomet. Chem. 692 (2007) 5307–5316.

[11] W.-H. Sun, K. Wang, K. Wedeking, D. Zhang, S. Zhang, J. Cai, Y. Li, Organometallics 26 (2007) 4781–4790.

[12] (a) S. Vangapandu, M. Jain, R. Jain, S. Kaur, P.P. Singh, Bioorg. Med. Chem. 12 (2004) 2501–2508;
(b) U. Jordis, F. Sauter, M. Rudolf, G. Cai, Monatsh. Chem. 119 (1988) 761–780;
(c) E.C. Riesgo, X. Jin, R.P. Thummel, J. Org. Chem. 62 (1996) 3017–3022.

[13] F. Lions, K.V. Martin, J. Am. Chem. Soc. 79 (1957) 2733–2738.

[14] A.M. Archer, M.W. Bouwkamp, M.-P. Cortez, E. Lobkovsky, P.J. Chirik, Organometallics 25 (2006) 4269–4278.

[15] L.P. Spencer, R. Altwer, P. Wei, L. Gelmini, J. Gauld, D.W. Stephen, Organometallics 22 (2003) 3841–3854.

[16] G.M. Sheldrick, SHELXTL-97, Program for the Refinement of Crystal Structures, University of Göttingen, Germany, 1997.